Geol. Mag. **141** (*3*), *2004, pp. 345–351.* © *2004 Cambridge University Press*
DOI: 10.1017/S0016756804009197 *Printed in the United Kingdom*

Linking Paleogene denudation and magmatic underplating beneath the British Isles

RICHARD TILEY, NICKY WHITE* & SULEIMAN AL-KINDI
Bullard Laboratories, Department of Earth Sciences, Madingley Rise, Madingley Road, Cambridge, CB3 0EZ, UK

(*Received* 2 September 2002; *revised version received* 15 January 2004; *accepted* 15 January 2004)

Abstract – A simple flexural model is used to explore the relationship between magmatic underplating and denudation. First, we show how denudation can be calculated as a function of underplating. The distribution and density of underplate are obviously important parameters in determining the wavelength and amplitude of denudation. However, the denudational pattern can be considerably modulated by the flexural rigidity of the lithosphere. Several other parameters also play a significant role. For example, we show how variations in pre-existing bathymetry and in present-day topography affect denudational calculations. We have applied our simple algorithm to the problem of Paleogene underplating beneath the British Isles. Forward and inverse modelling of travel-time data from a wide-angle seismic experiment which traversed the British Isles suggests that a large pod of high velocity material occurs at Moho depths beneath the Irish Sea. The shape and inferred density of this pod are used to calculate the amplitude and wavelength of denudation for different flexural rigidities. We compare our predictions with the observed pattern of Paleogene denudation and conclude that the bulk of the observed denudation can be accounted for by magmatic underplating associated in a general way with the Iceland Plume. Notwithstanding this agreement, there is compelling evidence for additional mild uplift events especially during the Neogene. These mild events may reflect fluctuating dynamic topography associated with the Iceland Plume.

Keywords: magmatic underplating, denudation, British Isles, Paleogene.

1. Introduction

There is considerable interest in mechanisms which explain regional epeirogenic uplift and denudation. This long-wavelength form of uplift can be divided into two categories: transient and permanent. Transient uplift is probably generated by temporal and spatial variations in mantle convection. Therefore an ability to map transient uplift through space and time would have important implications for convective dynamics. Permanent epeirogenic uplift is thought to be mainly generated by magmatic underplating, although under certain circumstances lower crustal flow might play a role. There may be other mechanisms for generating transient and permanent uplift but convection and underplating can be regarded as the principal ones (Cox, 1993).

There are two important difficulties when attempting to measure epeirogenic uplift. First, it is not easy to discriminate between permanent and transient uplift although the relationship between free-air gravity anomalies and topography in the frequency domain can sometimes be of use (Tiley, McKenzie & White, 2003). Secondly, it is difficult to measure epeirogenic uplift either at present or during the past. At the present day, topography does not necessarily equate with epeirogenic uplift since crustal thickness variation generated in many different ways will produce topography. In the geological record, the problem becomes more complicated because uplift must usually be inferred from the pattern of denudation. Denudation itself is difficult to measure accurately and estimates are usually no better than ± 0.5 km (e.g. Rowley & White, 1998).

Here we examine the relationship between denudation and magmatic underplating. Our principal aim is to develop a simple model which links observed denudation and inferred underplating. In this way, we should be able both to test the underplating hypothesis and isolate components of denudation which can be attributed to, say, transient epeirogeny. After describing and testing our model, we apply it to a region which encompasses the British Isles.

2. Underplating model

It is now generally accepted that magmatic underplating is an important mechanism for causing rapid epeirogenic uplift of the continents and their margins. For 30 years, the existence of underplating has principally been inferred by petrological and geochemical arguments (e.g. Cox, 1993). More recently, dense wide-angle seismic experiments have played an important role in delineating the thickness and extent of underplating, especially at continental margins (White & McKenzie, 1989).

* Author for correspondence: nwhite@esc.cam.ac.uk

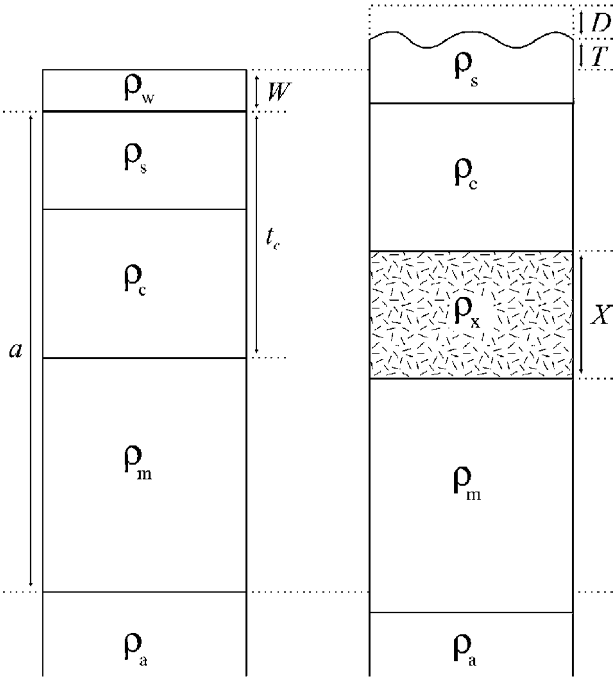

Figure 1. Cartoon which illustrates the isostatic consequences of magmatic underplating. Left-hand panel: column of lithosphere in equilibrium with mid-oceanic ridge and underlain by asthenosphere with density ρ_a; $W = B =$ thickness of water layer with density ρ_w; $t_c =$ thickness of crust which consists of sedimentary layer with density ρ_s on top of layer with density ρ_c; $a - t_c =$ thickness of lithospheric mantle with density ρ_m. Right-hand panel: column of lithosphere after injection of magmatic underplating of thickness X and density ρ_x; $D =$ partial denudation consequent upon uplift generated by magmatic underplating; $T =$ residual uplift (present-day topography); all other symbols as in left panel.

Here, we assume that magma is instantaneously intruded into continental lithosphere which is in isostatic equilibrium with the mid-oceanic ridge system (Fig. 1). Underplate is placed at the Moho although, in the absence of phase changes, its precise distribution within the lithosphere need not concern us.

If we assume Airy isostasy and if the top of the lithosphere remains at the reference level before and after underplating, the denudation, D, is given by

$$D = \left(\frac{\rho_a - \rho_x}{\rho_a - \rho_s}\right) X \qquad (1)$$

Other parameters are listed in Table 1. Provided the density of underplate is less than the density of the asthenosphere, Equation (1) shows that uplift and consequent denudation always occur. Thus if 5 km of underplate with a density of 2.9 Mg m^{-3} is emplaced, the top of the lithosphere is uplifted by 450 m. Erosion will amplify this uplift into 1.85 km of denudation or removal of rock.

We can refine this simple equation in two important ways. First, the elastic response of the lithosphere to loading is included. Secondly, the existence of topography and/or bathymetry both before and after the underplating event is incorporated.

Table 1. Parameters used in text (see also Turcotte & Schubert, 1982)

Symbol	Parameter	Value
a	Lithospheric thickness	120 km
t_c	Crustal thickness	30 km
X	Underplate thickness	km
B	Prior water depth	km
T	Residual topography	km
D	Denudation	km
ρ_w	Density of water	1 Mg m^{-3}
ρ_s	Density of sediment	2.4 Mg m^{-3}
ρ_c	Density of crust	2.8 Mg m^{-3}
ρ_m	Density of lithospheric mantle	3.33 Mg m^{-3}
ρ_a	Density of asthenosphere	3.2 Mg m^{-3}
ρ_x	Density of underplate	Mg m^{-3}
F	Flexural rigidity	Nm
T_e	Elastic thickness	km
w	Deflection	km
g	Gravitational acceleration	9.8 m s^{-2}
E	Young's Modulus	7×10^{10} Pa
ν	Poisson's Ratio	0.25

The deflection, w, which results from a load, is calculated using the thin sheet approximation which assumes that w is independent of depth (Turcotte & Schubert, 1982). The relationship between a vertical load, S, and w is given by

$$\left[\frac{F}{g}\nabla^4 + (\rho_a - \rho_w)\right] w = -\Delta\rho S \qquad (2)$$

where $\Delta\rho$ is the density contrast at the interface where the load is added. Other parameters are listed in Table 1. If the load is positive, then the deflection, w, will be negative (downwards). We assume that F is constant and that no horizontal forces act upon the lithosphere. These assumptions could easily be relaxed if better resolved denudation measurements became available but we see no reason to use a more complicated model at the moment.

In our case, we will assume that the deflection is equal to the denudation. Since underplating normally causes denudation, we require that a positive load generate a positive deflection. If we also allow for prior bathymetry, B, and residual topography, T, we obtain

$$\left[\frac{F}{g}\nabla^4 + (\rho_a - \rho_s)\right] w = (\rho_a - \rho_x)X - (\rho_a - \rho_w)B - \rho_a T \qquad (3)$$

Equation (3) assumes that the surface deflection (denudation) tends to zero if the flexural rigidity of the lithosphere becomes arbitrarily large. If $F = 0$, we obtain the Airy expression for denudation (White & Lovell, 1997).

Equation (3) is easily solved for periodic loads. If $\bar{w}$, $\bar{X}$, $\bar{B}$ and $\bar{T}$ are the Fourier transforms of w, X, B

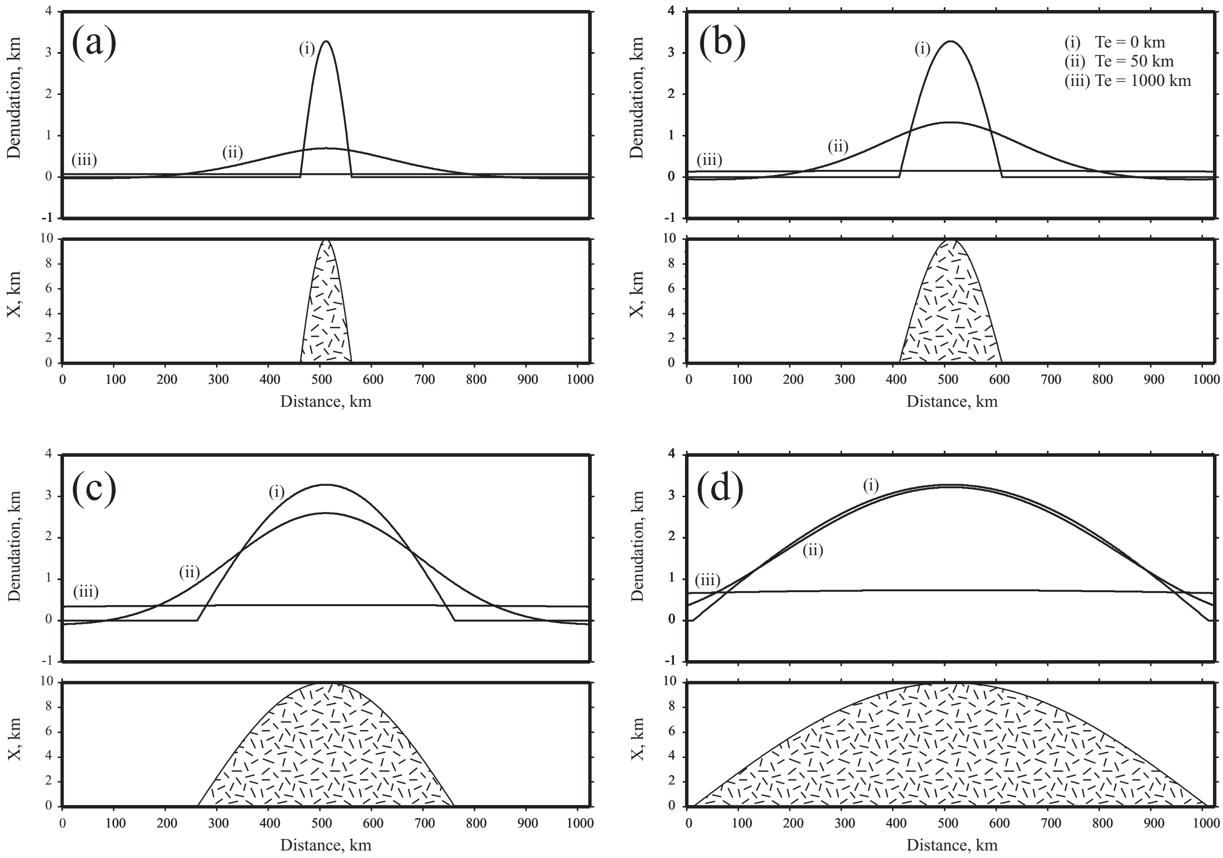

Figure 2. Denudation calculated for different elastic thicknesses. (a) Lower panel shows spatial distribution of magmatic underplating (maximum thickness = 10 km; width = 100 km); upper panel shows resultant denudation for three values of T_e, the elastic thickness (0, 50 and 1000 km). (b), (c) and (d) show the effects of increasingly wide distributions of magmatic underplating (200, 500 and 1000 km).

and T then

$$\bar{w} = \frac{[(\rho_a - \rho_x)\bar{X} - (\rho_a - \rho_w)\bar{B} - \rho_a \bar{T}]}{\left[\frac{Fk^4}{g} + (\rho_a - \rho_s)\right]} \quad (4)$$

where $k = 2\pi/\lambda$. If $k \to 0$ (that is the wavelength of the periodic load increases) or if $F \to \infty$, $\bar{w}$ tends to the Airy isostatic approximation. If $k \to \infty$ or $F \to 0$, $\bar{w} \to 0$ as required. We are conscious that different stress-free conditions can be applied (e.g. as $k \to \infty$, $\bar{w} \to S - B - T$). From a geological perspective, we think that it is more reasonable to infer that increasing flexural rigidity generates less denudation for a given distribution of underplate. F is usually converted into elastic thickness, T_e, using

$$F = \frac{ET_e^3}{12(1 - \nu^2)} \quad (5)$$

Equation (4) can be solved for different shapes of underplate by using a Fast Fourier Transform (Press *et al*. 1992). In Figures 2 and 3, we show how varying the different input parameters listed in Table 1 leads to different denudation patterns. First, we examine how denudation varies with load width and elastic thickness (Fig. 2). Narrow loads generate localized uplift and denudation if T_e is zero or very small. For even modest values of T_e, denudation is considerably reduced and spread out. As T_e becomes arbitrarily large, denudation always tends to zero. For wider loads, the difference between T_e of 0 and, say, 50 km is very small (Fig. 2d).

The effects of varying all other parameters are shown in Figure 3. Changes in the thickness and density of underplate have a predictable effect: as density decreases and thickness increases, the amount of denudation increases. Parts c and d of Figure 3 show clearly how sensitive denudation calculations are to variations in prior bathymetry and in residual topography. For example, a 500 m increase in water depth produces the same effect as reducing underplating thickness by 5 km. Such sensitivity is caused by the density contrasts in the isostatic equation: $(\rho_a - \rho_w)$ is nearly one order of magnitude greater than $(\rho_a - \rho_x)$.

3. Application

During Early Cenozoic times, initiation of the Iceland plume combined with opening of the North Atlantic Ocean generated enormous volumes of melt which were extruded and intruded along the fringing continental margins (e.g. White & McKenzie, 1989). A

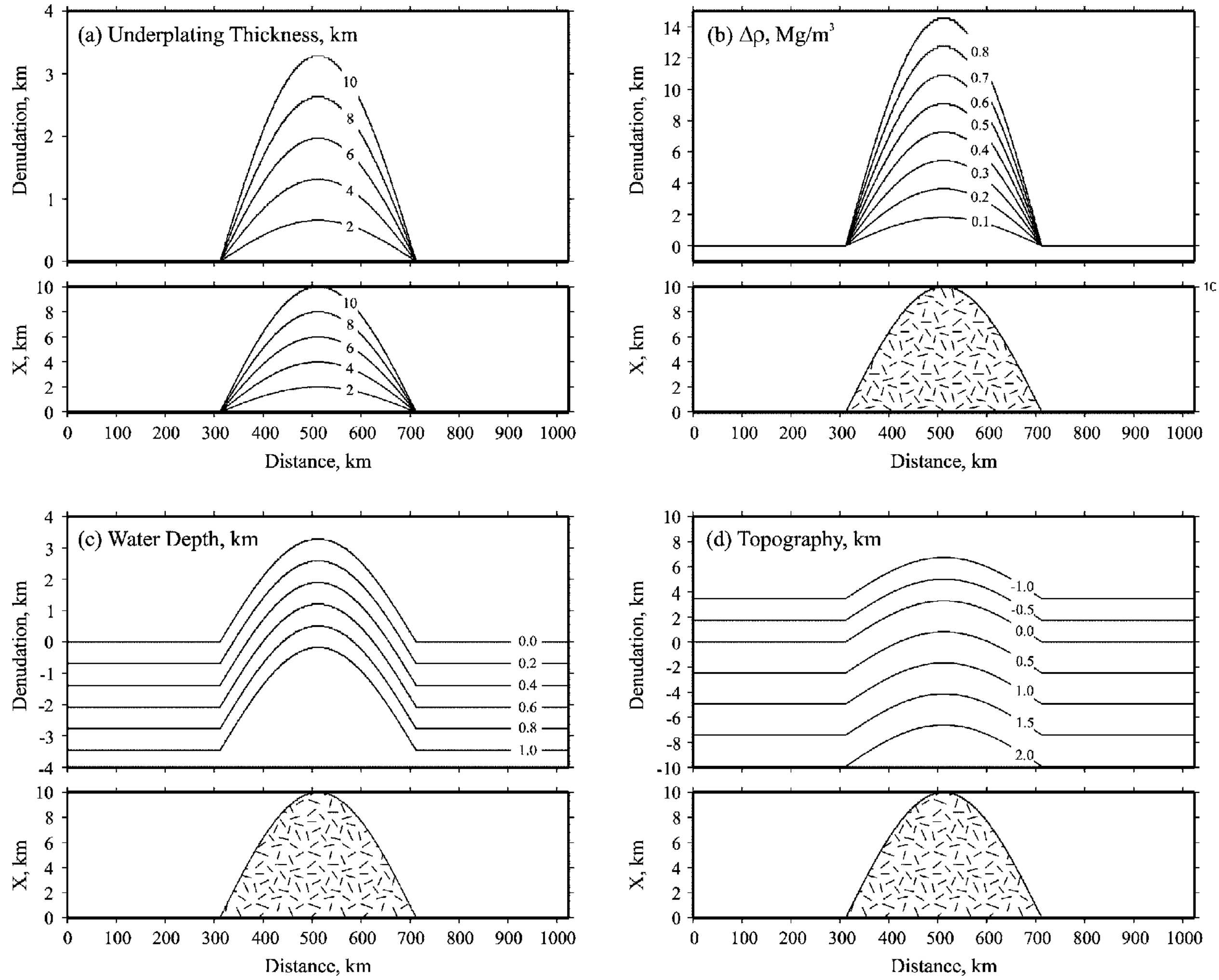

Figure 3. Denudation calculated for different configurations of magmatic underplating and for different initial/final conditions. (a) Lower panel shows spatial distribution of underplating (width = 400 km; maximum thickness varies from 2–10 km); upper panel shows resultant denudation assuming Airy isostasy. (b) Effect of varying density contrast between underplating and asthenosphere ($\Delta\rho = 0.1$–0.8. (c) Effect of varying initial water depth ($B = 0$–1 km). (d) Effect of varying present-day topography ($T = -1$–2 km).

significant amount of melt was also intruded at right angles to the nascent margins along a trajectory which runs from Disko Island through Iceland and Western Scotland down to Lundy. It is generally accepted that magmatic underplating at the extending continental margins had an important effect on vertical motions by suppressing extension-related subsidence. However, it is difficult to measure denudation at these margins because of large uncertainties in palaeobathymetry.

In order to investigate the relationship between denudation and magmatic underplating, we will focus our attention on a region where the effects of underplating have not been complicated by lithospheric stretching. The obvious choice is a region encompassing the British Isles which has a well-documented history of Paleogene magmatism and denudation.

Cenozoic denudation of the British Isles and surrounding regions has been measured in a range of different ways (for a summary, see Rowley & White, 1998). The best-known methods exploit the thermal history of sedimentary and upper crustal rocks by modelling vitrinite reflectance measurements and fission track data. Other methods include sonic velocity analysis and remnant subsidence modelling. Each of these four methods yields denudation values which do not generally agree. Remnant subsidence modelling usually provides lower-bound estimates due to uncertainties in rifting histories and in compaction. The trade-off between geothermal gradient and denudation generally means that the two thermal methods may overestimate denudation. Sonic velocity analysis gives denudation values with large uncertainties. These discrepancies suggest that at the moment denudation cannot be determined to better than about ± 0.5 km (Doré *et al.* 2002).

Jones *et al.* (2002) synthesized all denudation measurements based on vitrinite, subsidence and fission track data for a region which encompasses the British Isles (Fig. 4). Their map shows that 0.5–2 km of denudation occurred in a region which includes

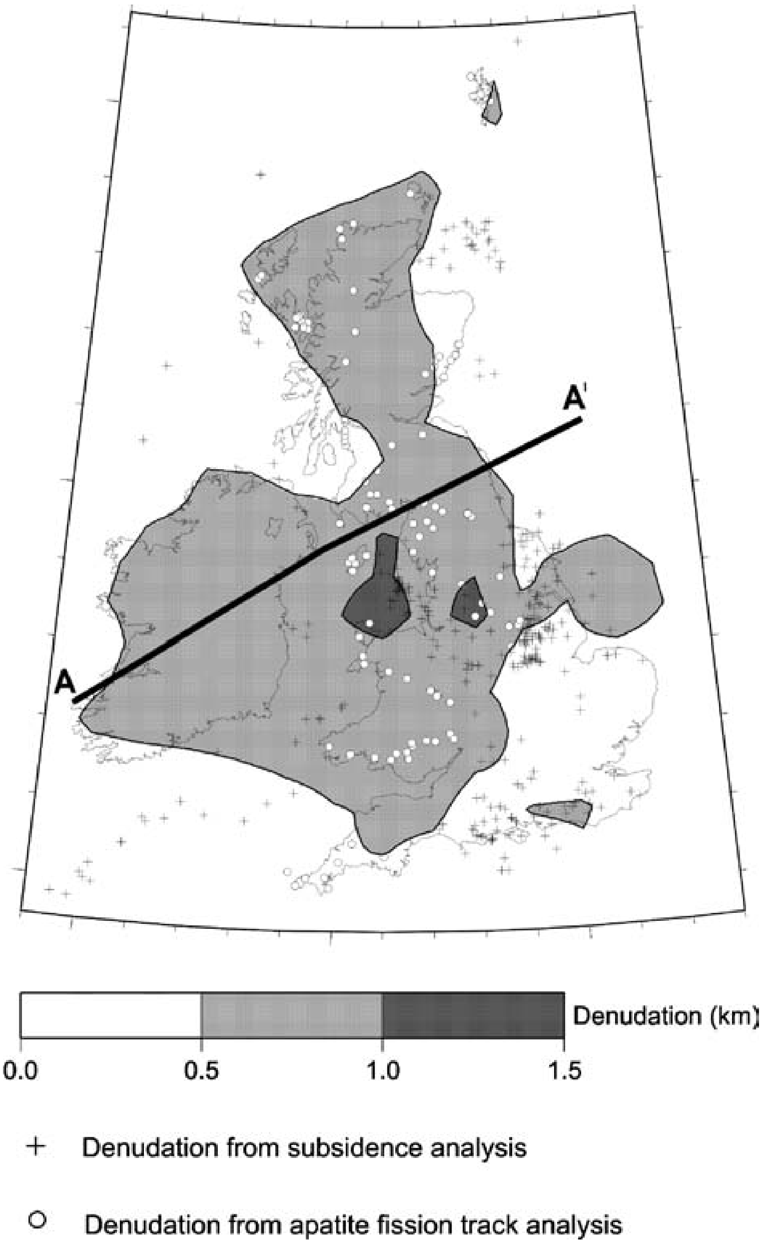

Figure 4. Map of British Isles which shows distribution of Paleogene denudation (see Jones *et al*. 2002, for further details). Line A–A′ is location of combined CSSP/ICSSP wide-angle seismic profile modelled by Al-Kindi *et al*. (2003). Prepared using Generic Mapping Tools (Wessel & Smith, 1995).

Scotland, Wales and the Irish Sea. The largest amounts of denudation occurred in the East Irish Sea and West Midlands of England where up to 3 km may be missing in places. Fission track data suggest that denudation mostly occurred during the Paleogene, although there is undeniable evidence for later, milder, denudational events (Green, Duddy & Hegarty, 2002). The record of clastic deposition in sedimentary basins such as the North Sea basin, the Faroe–Shetland basin and the Porcupine basin confirms that the greatest denudation occurred in the Paleogene. Jones *et al*. (2002) have also shown that the inferred volume of denuded material is broadly in agreement with the volume of Paleogene deposits. This agreement suggests that the pattern of Paleogene denudation is generally correct.

Brodie & White (1995) argued that Paleogene denudation was best accounted for by regional magmatic underplating. There is excellent evidence for mild shortening at different stages of the Cenozoic but the total amount of such shortening is several orders of magnitude smaller than that required to account for the measured denudation. More recently, Al-Kindi *et al*. (2003) have analysed data from a wide-angle seismic experiment which crosses Britain and Ireland (see Fig. 4 for location). Forward and inverse modelling of travel-time picks show that a pod of high velocity

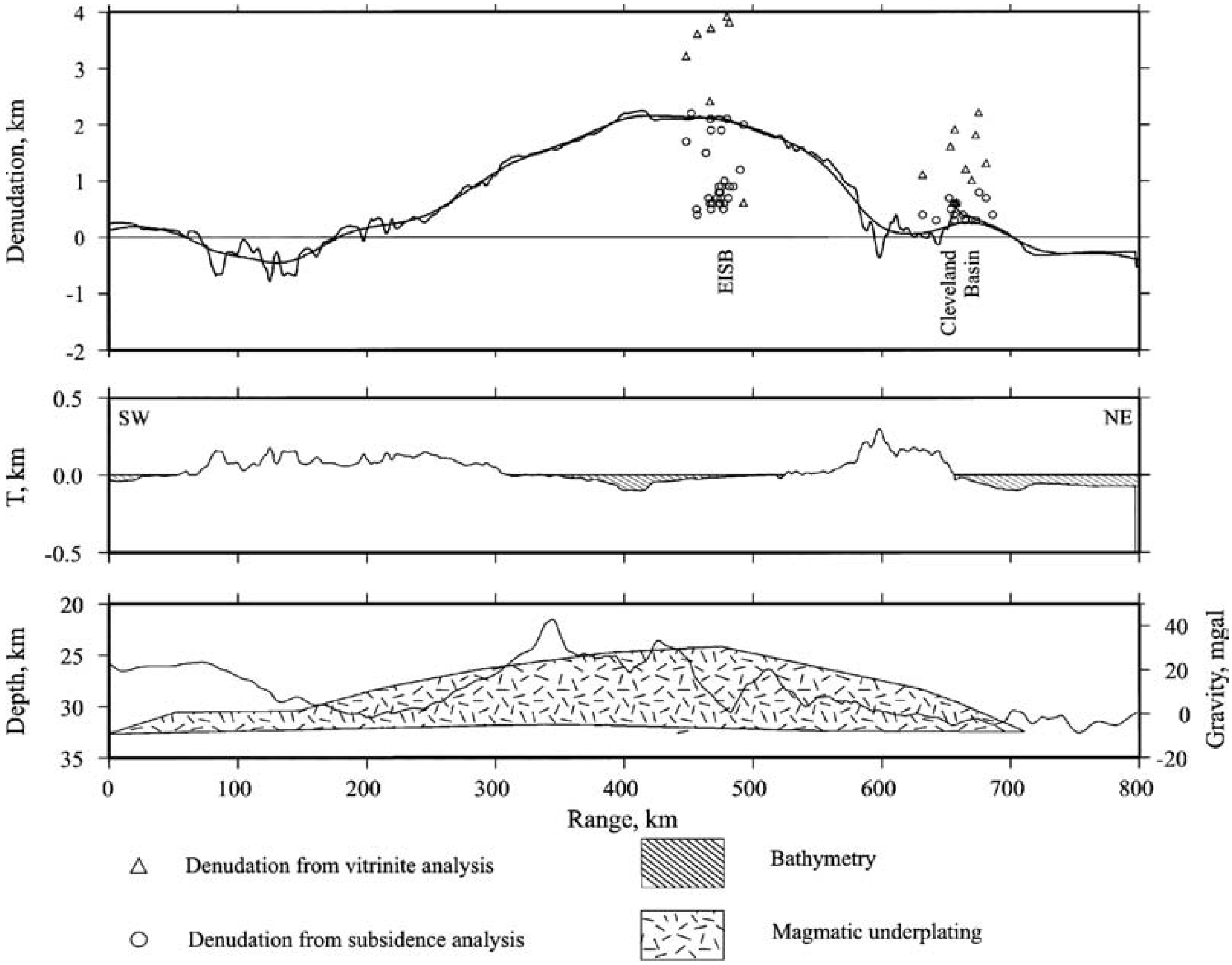

Figure 5. Observed and calculated denudation along Line A–A′ (see Fig. 4 for location). Upper panel: rough solid line = denudation calculated from distribution of magmatic underplating shown in lower panel, assuming $T_e = 0$ km; smooth solid line = denudation calculated from distribution of magmatic underplating shown in lower panel, assuming $T_e = 4$ km. EISB = East Irish Sea Basin. Middle panel: topography and bathymetry along Line A–A′. Lower panel: distribution of magmatic underplating along Line A–A′ determined from wide-angle modelling by Al-Kindi *et al*. (2003); solid line = free-air gravity anomaly along Line A–A′.

material occurs above the Moho. This pod is 8 ± 1 km thick directly beneath the Isle of Man. It thins towards the northeast, pinching out about half-way across England. It also thins to the southwest although there is insufficient ray coverage to determine whether or not it pinches out in Ireland. Al-Kindi *et al*. (2003) show that the velocity of the pod varies from 7.2 to 7.6 km s^{-1}. These velocities are consistent with an average density of ~ 2.9 Mg m^{-3}. Figure 5 shows that their high density pod has a clear long-wavelength gravity signature, especially at a range of 200–500 km. Igneous dyke swarms have been mapped throughout the Irish Sea.

The relationship between Paleogene denudation and the geometry of the high density pod can be investigated using our simple flexural model. Our starting point was the crustal density distribution inferred by Al-Kindi *et al*. (2003). The initial lithospheric template during Late Cretaceous times is shown in Figure 1. We assume that Late Cretaceous water depth was a constant 150 m along Line A–A′. This conservative assumption means that the calculated denudation is an underestimate. The present-day topography is equated with residual topography. In other words, we assume that there has been no epeirogenic uplift or subsidence since the injection of underplate. This assumption is undoubtedly wrong since there is excellent evidence for epeirogenic uplift events in the Oligocene–Miocene and in the Pliocene (Doré *et al*. 2002). However, we maintain that these events have a much smaller amplitude than that which occurred in the Paleogene. The GTOPO30 topographic database is accurate to ± 30 m at the 90 % confidence level which introduces an error of ± 100 m. Late Cretaceous water depth is far less well constrained and so is a more significant source of error.

Calculated denudation profiles can be compared with denudation data which have been projected onto Line A–A′ (Fig. 5). Our results show that there is broad agreement between predicted and observed denudation for a range of values of T_e. The calculated denudation over the region of maximum underplating matches data from the East Irish Sea reasonably well. Note that vitrinite reflectance data tend to yield overestimates of denudation, whereas remnant subsidence data tend to yield underestimates. Data from the Cleveland Basin also match the calculated denudation.

From a denudational point of view, the difference between an elastic thickness of zero and 5 km is negligible. However, an independent study of the spectral relationship between free-air gravity anomalies and topography suggests that T_e is ~ 5 km (Tiley, McKenzie & White, 2003). Changes in Late Cretaceous water depth have a much greater effect on the misfit. We found that this misfit is minimized for a water depth of 100–150 m but we do not mean to imply that palaeowater depths should be constrained in this way!

An important question raised by this analysis is the configuration of present-day topography. Our results suggest that the largest amount of underplating and consequent denudation occurred directly beneath the Irish Sea. This region has minimal topographic expression today. Instead, the largest present-day topography on Line A–A′ occurs either in eastern England where Paleogene underplating was modest or in southwest Ireland where underplating is either negligible or absent. One possible explanation is that the present-day topography in northern England and in southwest Ireland was generated by a phases of later, milder, epeirogenic uplift. Jones *et al*. (2002) have suggested that the long-wavelength gravity anomaly over these islands is evidence for present-day dynamic support of topography. The spatial relationship between this dynamic support and present-day topography is obscure and undoubtedly depends upon the variation of dynamic support through time.

In summary, we describe a two-dimensional model for calculating denudation profiles from given distributions of magmatic underplating. Synthetic modelling is used to explore the effects of underplating density, underplating geometry, flexural rigidity and topography. We show that the pattern of previously existing topography or bathymetry has a significant influence on calculated denudation. Our simple algorithm was then applied to a region encompassing the British Isles where there is evidence for coupled denudation and magmatic underplating during Paleogene times. The general agreement between predicted and observed denudation suggests that Cenozoic epeirogeny was primarily, but not exclusively, driven by a magmatic underplating event.

Acknowledgements. A Natural Sciences Tripos Part III project carried out by RT formed the basis of this paper. The British Geological Survey and the Dublin Institute for Advanced Studies generously permitted access to their digital gravity dataset. We are grateful to S. Jones and D. Lyness for their help. J. Cartwright and R. England provided very constructive and thorough reviews. This paper was written while NW was a visiting professor at Institut de Physique du Globe, Paris. He thanks C. Jaupart and S. Singh for their help and hospitality. Department of Earth Sciences Contribution no. 7407.

References

AL-KINDI, S., WHITE, N., SINHA, M., ENGLAND, R. & TILEY, R. 2003. The trace of a hot convective sheet. *Geology* **31**, 207–10.

BRODIE, J. & WHITE, N. 2995. Sedimentary basin inversion caused by igneous underplating: Northwest European continental shelf. *Geology* **22**, 147–50.

COX, K. G. 1993. Continental magmatic underplating. *Philosophical Transactions of the Royal Society, London* **A342**, 155–66.

DORÉ, A. G., CARTWRIGHT, J. A., STOKER, M. S., TURNER, J. P. & WHITE, N. (eds) 2002. *Exhumation of the North Atlantic margin: timing, mechanisms and implications for petroleum exploration.* Geological Society of London, Special Publication no. 196.

GREEN, P. F., DUDDY, I. R. & HEGARTY, K. A. 2002. Quantifying exhumation from apatite fission track analysis and vitrinite reflectance data: precision, accuracy and latest results from the Atlantic margin of NW Europe. In *Exhumation of the North Atlantic Margin: Timing, Mechanisms and Implications for Petroleum Exploration* (eds A. Doré, J. Cartwright, M. Stoker, J. Turner and N. White), pp. 331–54. Geological Society of London, Special Publication no. 196.

JONES, S. M., WHITE, N., CLARKE, B., ROWLEY, E. & GALLAGHER, K. 2002. Present and past influences of the Iceland plume on sedimentation. In *Exhumation of the North Atlantic Margin: Timing, Mechanisms and Implications for Petroleum Exploration* (eds A. Doré, J. Cartwright, M. Stoker, J. Turner and N. White), pp. 13–25. Geological Society of London, Special Publication no. 196.

PRESS, W. H., TEUKOLSKY, S. A., VETTERLING, W. T. & FLANNERY, B. P. 1992. *Numerical Recipes in FORTRAN.* Cambridge University Press, UK.

ROWLEY, E. & WHITE, N. 1998. Inverse modelling of extension and denudation in the East Irish Sea and surrounding areas. *Earth and Planetary Science Letters* **161**, 57–71.

TILEY, R., MCKENZIE, D. & WHITE, N. 2003. The elastic thickness of the British Isles. *Journal of the Geological Society of London* **160**, 499–502.

TURCOTTE, D. & SCHUBERT, G. 1982. *Geodynamics: applications of continuum physics to geological problems.* New York: John Wiley & Sons.

WESSEL, P. & SMITH, W. H. F. 1995. New version of the Generic Mapping Tools released. *EOS Transactions of the American Geophysical Union* **76**, 329.

WHITE, N. & LOVELL, B. 1997. Measuring the pulse of a plume with the sedimentary record. *Nature* **387**, 888–91.

WHITE, R. S. & MCKENZIE, D. 1989. Magmatism at rift zones: the generation of volcanic continental margins and flood basalts. *Journal of Geophysical Research* **94**, 7685–730.